The Journal of Physical Chemistry A

 VOLUME 103, NUMBER 20, MAY 20, 1999

LETTERS

A Theoretical Study of the Reaction of $ClONO_2$ with HCl on Ice

Roberto Bianco and James T. Hynes*

Department of Chemistry and Biochemistry, University of Colorado, Boulder, Colorado 80309-0215

Received: February 8, 1999

The direct $ClONO_2 + HCl \rightarrow Cl_2 + HNO_3$ reaction on ice, implicated in polar stratospheric ozone depletion, is studied quantum chemically on a model ice lattice comprising nine water molecules. The reaction path is calculated at the HF/(HW*,3-21G) level, using the Hay−Wadt effective core potential for Cl. At these geometries, energies are recalculated at the MP2/(SBK+*,6-31+G*) level, with the Stevens−Bash−Krauss effective core potential for Cl. HCl is found to be ionized in the reactant complex. The calculated reaction internal energy barrier, including zero-point energy correction, is 6.4 kcal/mol. The reaction mechanism involves proton transfer in the ice lattice, accompanied by nucleophilic attack of Cl^- on the $Cl^{\delta+}$ in $ClONO_2$; the lattice is an active participant in the reaction. Implications for heterogeneous atmospheric chemistry are discussed.

I. Introduction

Since the proposal[1,2] that ice particles in Antarctic polar stratospheric clouds could be responsible for the reactivation of chlorine from the so-called reservoir species $ClONO_2$ and HCl, numerous experimental studies[3] have demonstrated the remarkable efficiency of the reactions

$$ClONO_2 + HCl \rightarrow Cl_2 + HNO_3 \qquad (I.1)$$

$$ClONO_2 + H_2O \rightarrow HOCl + HNO_3 \qquad (I.2)$$

$$HOCl + HCl \rightarrow Cl_2 + H_2O \qquad (I.3)$$

on ice, strongly supporting the importance of these heterogeneous reactions in polar stratospheric ozone depletion. Among the central issues related to reactions I.1−I.3 is whether the net conversion of HCl and $ClONO_2$ occurs in one step, i.e., eq I.1, or in a two-step sequence, i.e., eq I.2, followed by eq I.3. While this remains under active experimental study, growing support has been given to the view that the direct one-step mechanism (eq I.1) is dominant under acidic conditions[4−7]—including and especially those due to HCl ionization—although its microscopic mechanism remains unclear.

Here we present a quantum chemical study of reaction I.1 on a model ice lattice,[8] via a $HCl{\cdot}ClONO_2{\cdot}(H_2O)_9$ cluster. As observed in the calculation described within, an acidic condition is realized via dissociation of HCl, a proton transfer from molecular HCl to a coordinated water molecule to form a $Cl^-H_3O^+$ contact ion pair (CIP), in the presence of $ClONO_2$. This observation is consistent with previous theoretical work[9] indicating HCl ionization at an ice surface.[10] In the present work, we study the reaction of $ClONO_2$ in the presence of this CIP. This contrasts with another real possibility in which the excess proton has transferred far from the $ClONO_2$ reaction site, such that the ice surface reaction would be

$$ClONO_2 + Cl^- \rightarrow Cl_2 + NO_3^- \qquad (I.4)$$

studied previously in the gas phase.[11] The eq I.1 vs eq I.4 issue has not been directly addressed experimentally, but an initial CIP scenario is supported by recent work[12] indicating that a

* Corresponding author. Fax +303 492 5894. E-mail: hynes@spot.colorado.edu.

10.1021/jp990471b CCC: $18.00
Published on Web 05/01/1999

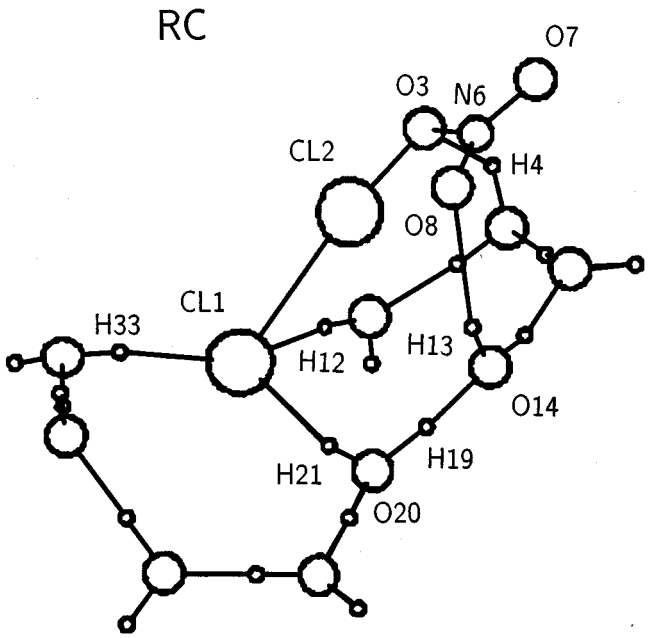

Figure 1. $H_3O^+ \cdot Cl^-$ $ClONO_2 \cdot (H_2O)_8$ reactant complex for the MP2 path. For RC, TS, and PC the reference frame has Cl1 as the origin, O14 along the positive *y* semiaxis, and Cl2 in the *yz* plane.

hydrated proton tends to remain in the neighborhood of an ice surface, and in any event it explicitly addresses the issue of acidic conditions at the ice surface. We will return to the alternate route (eq I.4) issue at the conclusion of this Letter.

In Section II, the model reaction system and computational strategy are presented. The reaction path is interpreted in Section III, while concluding remarks are offered in Section IV, in the context of heterogeneous atmospheric chemistry.

II. The $HCl \cdot ClONO_2 \cdot (H_2O)_9$ Model Cluster

We model the $HCl + ClONO_2$ reaction (eq I.1) along the lines of our study of the $ClONO_2$ hydrolysis (eq I.2) on ice.[13] There, the reaction system was represented as a $H_2O \cdot ClNO_2 \cdot (H_2O)_2$ cyclic complex (with additional water to better mimic the ice lattice). Here, we start with the $HCl \cdot ClONO_2 \cdot (H_2O)_2$ cyclic complex and, in anticipation that HCl should be ionized, expand the reaction cluster by seven extra waters (i) to provide sufficient solvation for the resulting $Cl^-H_3O^+$ CIP, and (ii) to mimic the local structure of an ice crystal basal plane face by maintaining the solvating waters in place during the reaction. A representative structure of the $HCl \cdot ClONO_2 \cdot (H_2O)_9$ system is shown in Figure 1.

For all calculations we have used the quantum chemistry suite of programs GAMESS.[14] Due to the considerable model reaction system size, we adopt the IRCMax procedure, successful in other contexts:[15] the Intrinsic Reaction Coordinate (IRC) path[16] is calculated at the HF level, with energies recalculated at the MP2 level for the optimized geometries along the path. All atoms except Cl are described with 3-21G[17] and 6-31+G*[18] basis sets at the HF and MP2 levels, respectively. We use effective core potentials (ECPs) for Cl: the Hay−Wadt (HW)[19] ECP, compatible with a −21 split valence basis, and the Stevens−Bash−Krauss (SBK)[20] ECP, compatible with a −31 split valence basis, for the HF and MP2 calculations, respectively. In the MP2 calculations, the common polarization exponent for O and N is 0.8,[21] while the diffusion exponents are 0.0845 (O) and 0.0639 (N).[22] The Cl polarization and diffusion exponents are 0.75[21] and 0.0483,[23] respectively, used in both HF and MP2 calculations. The two levels of calculations are denoted HF/(HW*,3-21G) and MP2/(SBK+*,6-31+G*)//HF/(HW*,3-21G), henceforth simply referred to as HF and MP2, respectively.

III. $HCl \cdot ClONO_2 \cdot (H_2O)_9 \rightarrow Cl_2 + NO_3^- \cdot H_3O^+ \cdot (H_2O)_8$

In this section, we describe the calculation of the HF IRC path, its MP2 energy correction, and the character of the reactant complex (RC), transition state (TS), and subsequent features resulting from the MP2 calculation.

A. HF IRC Path. The calculation of the IRC path requires structure and frequencies of the TS. As in ref 13, we have optimized the RC and then pulled the system uphill along a constrained minimum energy path toward the TS by decreasing the Cl−Cl distance stepwise and optimizing all remaining internal coordinates at each step.

Access to the TS region, as signaled by a sufficiently low energy gradient, was not reflected by the frequency calculation—due to the numerous "soft" water network modes of the reaction system—which yielded several imaginary frequencies, none representative of an expected nucleophilic attack, thus preventing attempts to locate the TS.

This difficulty was circumvented in two steps. First, the products' side of the reaction path adjacent to the TS region was accessed by further reducing the Cl−Cl distance and optimizing the cluster's structure, and the IRC path toward the products calculated with a step of 0.1 au (amu$^{1}/_{2}$ bohr). Structure examination along the IRC path revealed the expected Cl_2 and NO_3^- ion formation, thus confirming that the TS region was the relevant one. A similar calculation on the reactants' side yielded the starting RC structure.

Then, noting the TS should involve the nucleophilic coordinate $R_{Cl-ONO_2} - R_{Cl-Cl}$, we calculated the potential energy surface (PES) as a function of R_{Cl-ONO_2} and R_{Cl-Cl} spanning the ranges delimited by their values in two optimized cluster structures bordering the TS region, on the reactants' and products' side. This PES mapping revealed a saddle, and a point close to the approximate saddle point provided an excellent guess to the TS full optimization (see Table 1S). The entire HF path was then recalculated with a 0.05 au stride.

B. HF IRC Path with MP2 Energy Correction. The MP2 energy profile is shown in Figure 2a, together with the quite similar preliminary HF energy profile. We now discuss in detail the reaction path's main features.

a. $H_3O^+ \cdot Cl^- \cdot ClONO_2 \cdot (H_2O)_8$ Reactant Complex. The RC structure corresponding to the MP2 minimum is displayed in Figure 1 (see Table 2S). A cycle involving $ClONO_2$, a $Cl^-H_3O^+$ CIP, and one other water molecule (O14) is evident. HCl has transferred a proton to the next water in the cycle (O20) producing the CIP, consistent with ref 9 and 24. The CIP is fully coordinated, as are all the hydrogens on the next water in the ring (O14).

$ClONO_2$ has Cl2 coordinated to the chloride ion Cl1, while O8 and O3 are H-bonded to the lattice. $ClONO_2$ is planar as in the gas phase,[25] a sign of the inability of the environment (inclusive of the Cl^- anion) to disrupt the electronic π delocalization, which evidently determines $ClONO_2$ planarity.[26] The Löwdin natural population analysis[28] partial charge is 0.42*e* on Cl2 (an important electropositive feature) and −0.42*e* on the NO_3 group. The character of the $ClONO_2$ charge distribution argues against a view[7,29] of $ClONO_2$ on ice as ionized.

b. Transition State Region. With inclusion of the difference in zero-point energies (ZPE) of the RC and TS,[27] the MP2 barrier height is 6.4 kcal/mol. In order to understand the TS characteristics (see Table 3S), we discuss the reaction system evolution starting from the RC. The reaction path's initial stages

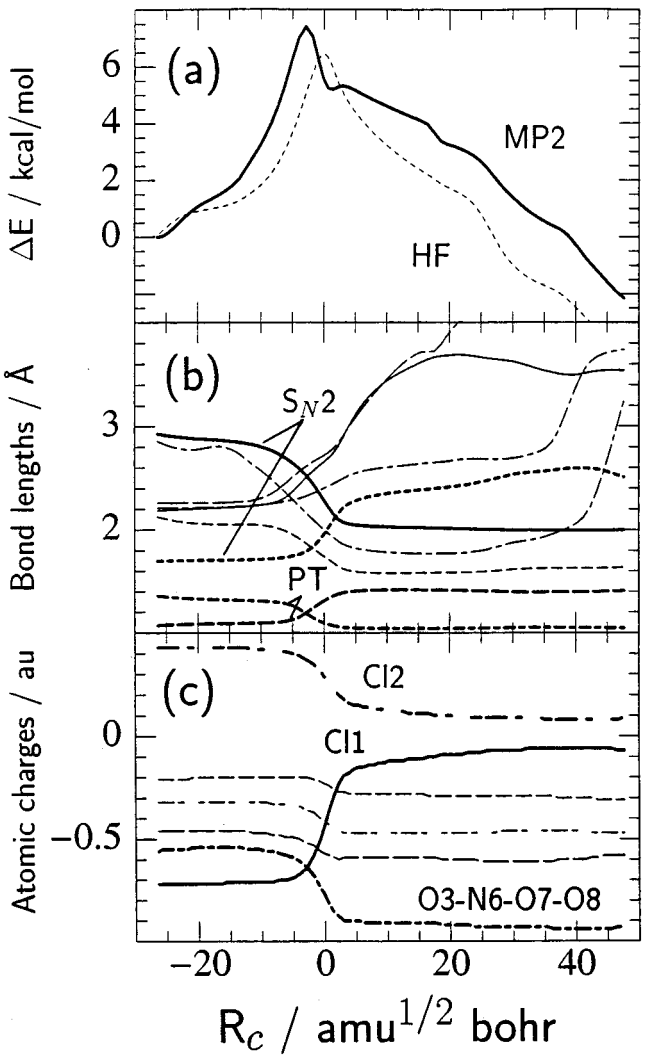

Figure 2. (a) MP2 (full, thick line) and HF (dashed, thin line) energies in kcal/mol along the HF IRC path. R_c is the distance along the HF IRC path in terms of the vector of mass-scaled cartesian coordinates for all atoms. $R_c \sim 0$ au labels the HF level transition state location. (b) Selected bond lengths in Å. On the leftmost side, starting from the top, labels are: Cl1−C12, O3−H4, Cl1−H12, Cl1−H33, Cl1−H21, O8−H13, Cl2−O3, O14−H19, and O20-H19 with numbering scheme as in Figure 1. For convenience, the curves involved directly in the S_N2 process (Cl1−Cl2 and Cl2−O3) and the proton transfer (PT) (O14−H19 and O20−H19) are labeled. For more detailed discussion, see the text. (c) Selected natural population analysis atomic partial charges in au from the HF/(SBK+*,6-31+G*) wavefunction during the MP2 calculation. On the left side, starting from top, labels are q_{Cl2}, q_{O7}, q_{O8}, q_{O3}, $q_{NO_3^-}$, and q_{Cl1}. The important S_N2 subsystem groupings are labeled.

predominantly involve (i) increased solvation of the incipient nitrate leaving group and (ii) desolvation of the attacking chloride ion.

The most pronounced feature of the former is evident in Figure 2b, where after only very slight bond length changes in the system, the nitrate O3−H4 H-bond begins shortening at $R_c \sim -15$ au. This large-amplitude bond shrinking at the oxygen in the nucleophilic Cl1−Cl2−O3 axis is accompanied by a larger MP2 energy increase along the path (Figure 2a), and is an important feature along a significant portion of the remaining path. Near $R_c \sim -9$ au, further nitrate solvation commences by H-bond strengthening at O8−H13, i.e., the nitrate group oxygen external to the Cl1−Cl2−O3 system axis. The second feature, chloride ion Cl1 desolvation, initiates at $R_c \sim -9$ au, with weakening of its H-bonds with H21, H12, and, to a lesser degree,

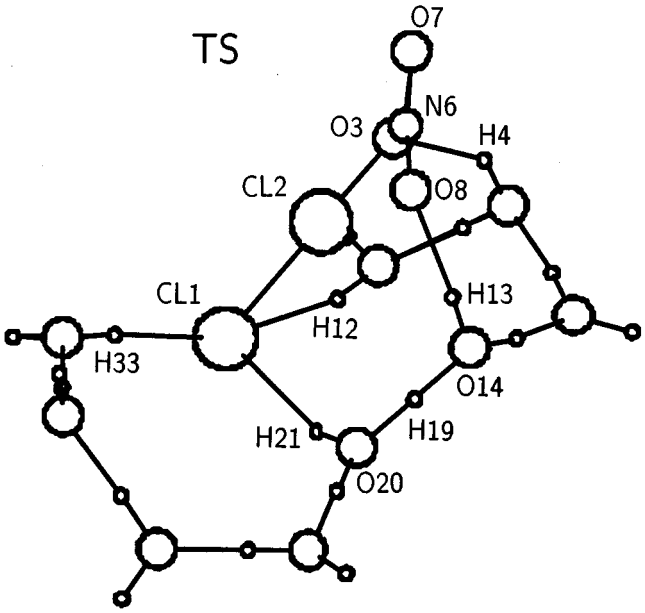

Figure 3. MP2 path transition state, $R_c \sim -2.88$ au. Atom numbering scheme and definition of reference frame as in Figure 1. See text for discussion.

H33. In particular, the first signals the onset of an important proton transfer in the lattice, discussed below. All these preliminary ($R_c < -9$ au) solvation/desolvation features occur without any significant change in the charge distribution of the $Cl^-\cdots Cl^{\delta+}\cdots ONO_2^{\delta-}$ system (cf. Figure 2c), a characteristic in common with solution phase S_N2 reactions.[30] While Cl1 has begun its approach to Cl2, both its charge and the Cl2−O3 bond length remain those of the RC.

The immediate vicinity of the TS ($R_c \sim -2.88$ au) involves a continuation of the motions previously identified, and in particular the proton transfer of H19 from O20 to O14; indeed, the crossing of the O14−H19 and O20−H19 bond length curves (Figure 2b) coincides with the TS peak in the MP2 energy (Figure 2a).[31] The MP2 TS structure, displayed in Figure 3, clearly reveals this proton transfer feature within the lower portion of the cycle connecting Cl1 and O8 via O20 and O14.

Despite this TS identification, it is too simplistic to view the critical TS region features solely in terms of the proton transfer. In particular, it is clear from Figure 2, parts b and c, that the S_N2 aspects of the reaction—the charge shifting from the attacking chloride Cl1 to the leaving nitrate group and the associated compression of the forming molecular chlorine bond Cl1−Cl2 and breaking of the Cl2−O3 bond—are simultaneously in train and then very rapidly complete. The transferring proton has an important *electronic* influence in assisting this S_N2 process: its TS region location allows it to act on both the nucleophile and the leaving group by (i) weakening the H-bonds to Cl1 [see curves for Cl1−H12, Cl1−H21, Cl1−H33 in Figure 2b], thus making the Cl1 electrons more available for its nucleophilic attack role, while (ii) further engaging the lone pairs of the nitrate group via the H_3O^+-strengthened O8−H21 and O3−H4 H-bonds, assisting its leaving group role. The former of these two last H-bonds, involving H_3O^+ directly, weakens the Cl2−03 bond (two bonds away) mostly via the NO_3^- π electron system, while the latter, indirectly strengthened by H_3O^+ via polarization of the water network, acts directly on one of the O3 lone pairs, thus drawing on the Cl2−O3 electron density and weakening this bond.

In one extreme, sequential view, the proton transfer (PT) induces the S_N2 reaction; in another extreme view, the PT and

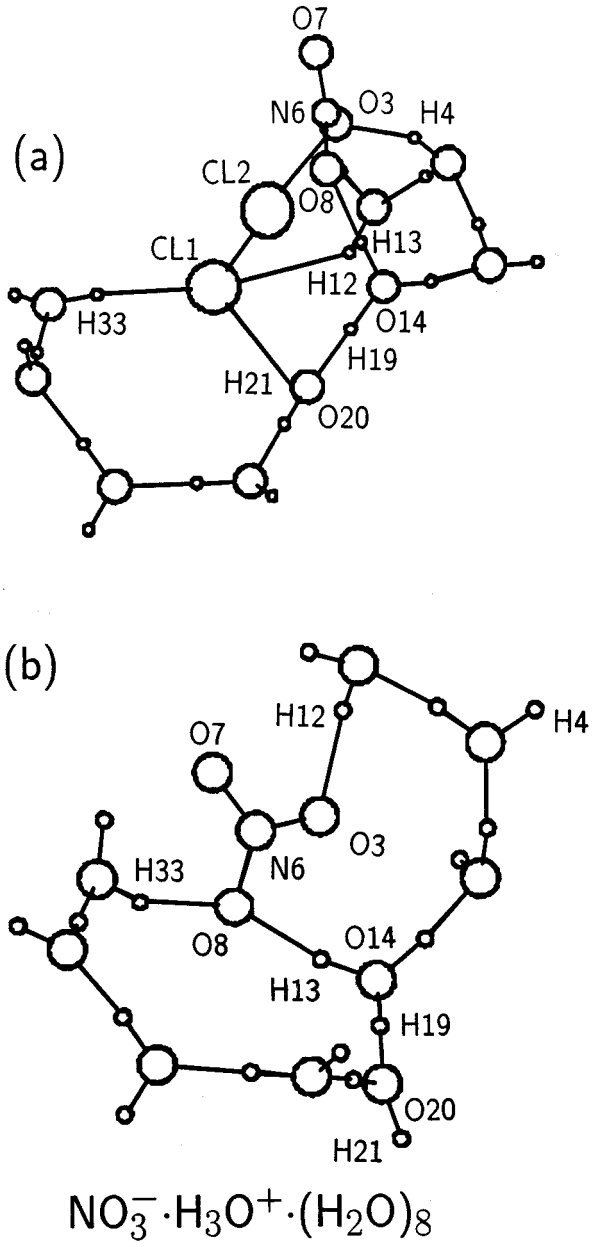

Figure 4. MP2 path product region. (a) Products' side complex showing Cl_2 formation. $R_c \sim 5.42$ au. (b) Relaxed $NO_3^- \cdot H_3O^+ \cdot (H_2O)_8$ complex (not reported on the MP2 path of Figure 2a). Atom numbering scheme and definition of reference frame as in Figure 1.

the S_N2 process are concerted. The present calculations depict an intermediate situation, e.g., Figure 2b,c indicate that the PT overlaps the S_N2 geometry change and charge shifting features, rather than being either distinctly separated or completely coincident. Further, the energy variation in the TS region is only a few kcal/mol. A fair characterization adequate for present purposes would be that the TS region involves a *coupled* PT/S_N2 process.

c. Product Region. Beyond the TS region, the subsequent reaction path is best described in several stages. Figure 4a reveals the formation of molecular Cl_2, together with the completed PT (see Table 4S). At this stage, a nitric acid contact ion pair $O_2NO^- \cdots H_3O^+$ is evident, involving O8−H13, as is a weak complex $Cl-Cl \cdots ONO_2^-$ involving a slightly polarized molecular chlorine ($q_{Cl} \sim 0.06e$; cf., Figure 2c).[32]

The remaining calculated reaction path retains the key features just described, but involves further lattice adjustments to optimize solvation of the nitric acid CIP and accomodate to the drastically decreased ionicity of Cl1. For example, Cl1's pattern of H-bonds is almost entirely disrupted, with cleavage of Cl1−H21 and Cl1−H33 and associated release of H12 apparent in Figure 2b. These rearrangements are not likely to occur in precisely this fashion on an ice surface, and so we do not present the detailed cluster path here; for example, the large-scale displacement of the H12-bearing water seems implausible in a real lattice, and incorporation of even further waters would be required to mimic ice lattice constraints. Unfortunately, this precludes a discussion of mechanistic details of the Cl_2 dissociation from ice, a topic left for future study. Nonetheless, we can estimate a net exothermicity by removing the molecular Cl_2 from the reaction cluster at $R_c \sim 47.63$ au and optimizing the resulting $NO_3^- \cdot H_3O^+ \cdot (H_2O)_8$ structure. The optimized solvated $NO_3^- H_3O^+$ CIP complex, shown in Figure 4b (see Table 5S), together with the energy of isolated molecular Cl_2 (see Table 6S), leads to an exothermicity, referenced to RC, of −11.4 kcal/mol.

IV. Concluding Remarks

The present modeling of the direct $HCl + ClONO_2$ reaction on an ice lattice to produce molecular chlorine and ionized nitric acid portrays a relatively facile coupled proton transfer/S_N2 mechanism, starting from a reactant complex in which HCl is ionized to produce a contact ion pair $H_3O^+Cl^-$ in the presence of molecular $ClONO_2$. These results support the early general suggestions[29] and subsequent views[4−7] of an ionic pathway, as opposed to a mechanism involving molecular HCl. The calculated mechanism shares with a previous prediction of the $ClONO_2$ hydrolysis[13] a crucial feature of proton transfer within a cyclic water network, such that the ice lattice is an *active* participant in the reaction.

While there is evidently no direct experimental measure of the $HCl + ClONO_2$ direct reaction rate available for comparison, the present results are certainly consistent with, for example, observations of "prompt" appearance of Cl_2 on a time scale of less than tens of milliseconds at 180−200 K.[6] Nonetheless, since proton transfer has been found above to be essential, a quantum proton motion treatment will be required for a more accurate activation energy assessment, and to estimate H/D kinetic isotope effects to provide a direct probe of the present mechanism.[33]

In the alternate two-step mechanism to produce Cl_2, the $ClONO_2$ hydrolysis (eq I.2) precedes eq I.3, and simply comparing the barrier heights estimated here for eq I.1, 6.4 kcal/mol, and in ref 13 for eq I.2, ca. 3 kcal/mol[34] might suggest that eq I.2 will be faster than eq I.1. But this is *not* the appropriate comparison in the acidic HCl environment. Beyond the complexation of the electropositive Cl in $ClONO_2$, stronger with a Cl^- than with a H_2O, the effects of an acidic environment in the $HCl + ClONO_2$ reaction are quite different from those on $ClONO_2$ hydrolysis. In the former, the strong H-bonding of the lattice waters to the nitrate group induced by H_3O^+ favors nucleophilic attack by weakening the nucleophilicity of the leaving group toward $Cl^{\delta+}$ (cf., Section IIIB.b); in the latter, the production of a transient hydroxyl-like nucleophile proposed critical for eq I.2[13] is hindered, strongly suppressing the hydrolysis.[35] These considerations support the dominance of the one-step mechanism (eq I.1) in an acidic HCl environment.

As noted in the Introduction, the simple S_N2 reaction route (eq I.4) involving only the chloride ion is a possibility if the excess proton in the $H_3O^+Cl^-$ CIP has been transported far from the $ClONO_2$ reaction site; while the present CIP scenario is

likely, the heterogeneous version of eq I.4 certainly cannot be dismissed. In ref 11, it was shown that eq I.4 is very fast in the gas phase, with no detectable barrier. However, as also noted in ref 11, a crucial issue is the surface analogue of the well-known liquid state solvation effects on S_N2 barrier heights;[36] the latter favor charge-localized reactant and product complexes over more charge-delocalized transition states, significantly increasing reaction barriers.[37] A dielectric continuum model suggested[11] that the resulting barrier for eq I.4 might be low at the ice surface, but the need for a molecular level description to clarify the issue was emphasized. Such calculations are underway to assess eq I.2 versus eq I.1 on ice[38] and in other environments.[4,39] Since proton transfer is not expected to be involved in eq I.4, experimental observation of an H/D kinetic isotope effect for the direct HCl + $ClONO_2$ reaction could provide support for the mechanism of eq I.1 found here; examination of DCl + $ClONO_2$ on D_2O ice would avoid complicating exchange issues.[40]

Acknowledgment. This work was supported by NSF grants ATM-9613802, CHE-9700419, and CHE-9709195. We thank Brad Gertner and Dave Hanson for many useful discussions.

Supporting Information Available: Tables 1S−6S with geometries, charges, and frequencies of relevant complexes as indicated in the text. This material is available free of charge via the internet at http://pubs.acs.org.

References and Notes

(1) Solomon, S.; Garcia, R. R.; Rowland, F. S.; Wuebbles, D. J. *Nature* **1986**, *321*, 755; Solomon, S. *Rev. Geophys.* **1988**, *26*, 131; *Nature* **1990**, *347*, 347.

(2) For reviews, see Brune, W. H.; Anderson, J. G.; Toohey, D. W.; Fahey, D. W.; Kawa, S. R.; Jones, R. L.; McKenna, D. S.; Poole, L. R. *Science* **1991**, *252*, 1260; Anderson, J. G.; Toohey, D. W.; Brune, W. H. *Science* **1991**, *251*, 39; Schoeberl, M. R.; Hartmann, D. L. *Science* **1991**, *251*, 46.

(3) See, for example, the review by Kolb, C. E.; Worsnop, D. R.; Zahniser, M. S.; Davidovits, P.; Keyser, L. F.; Leu, M.-T.; Molina, M. J.; Hanson, D. R.; Ravishankara, A. R.; Williams, L. R.; Tolbert, M. A. Laboratory studies of heterogeneous atmospheric chemistry. In *Advanced Series in Physical Chemistry, Vol. 3, Progress and Problems in Atmospheric Chemistry*; Barker, J. R., Ed.; World Scientific: Singapore, 1995; Chap. 18, p 771.

(4) Hanson, D. R.; Ravishankara, A. R. *J. Phys. Chem.* **1992**, *96*, 2682.

(5) Chu, L.T.; Leu, M.-T.; Keyser, L. F. *J. Phys. Chem.* **1993**, *97*, 12798.

(6) Oppliger, R.; Allanic, A.; Rossi, M. J. *J. Phys. Chem. A* **1997**, *101*, 1903.

(7) Horn, A. B.; Sodeau, J. R.; Roddis, T. B.; Williams, N. A. *J. Phys. Chem. A* **1998**, *102*, 6107.

(8) The gas-phase version of eq I.1 has a barrier of 45−64 kcal/mol, estimated in Mebel, A. M.; Morokuma, K. *J. Phys. Chem.* **1996**, *100*, 2985, which is obliterated by NO_3^- anion involvement (see also Van Doren, J. M.; Viggiano, A. A.; Morris, R. A. *J. Am. Chem. Soc.* **1994**, *116*, 6957).

(9) Gertner, B. J.; Hynes, J. T. *Science* **1996**, *271*, 1563; *Faraday Discuss.* **1998**, *110*, 301. See also Clary, D. C.; Wang, L. *J. Chem. Soc. Faraday Trans.* **1997**, *93*, 2763.

(10) For an extended discussion, see *Faraday Discuss.* **1996**, *100;* see also references in ref 9.

(11) Haas, B.-M.; Crellin, K. C.; Kuwata, K. T.; Okumura, M. *J. Phys. Chem.* **1994**, *98*, 6740.

(12) Cowin, J. P.; Tsekouras, A. A.; Iedema, M. J.; Wu, K.; Ellison, G. B. *Nature* **1999**, *398*, 405. The conclusion of this reference is consistent with that of some experimental HCl/ice work (see, for example ref 4), but evidently not with other work (Donsig, H. A.; Vickerman, J. C. *J. Chem. Soc. Faraday Trans.* **1997**, *93*, 2755; Horn, A. B.; Sully, J. *J. Chem. Soc. Faraday Trans.* **1997**, *93*, 2741).

(13) Bianco, R.; Hynes, J. T. *J. Phys. Chem.* **1998,** *102*, 309; Bianco, R.; Gertner, B. J.; Hynes, J. T. *Ber. Bunsen-Ges. Phys. Chem.* **1998,** *102*, 518.

(14) Schmidt, M. W.; Baldridge, K. K.; Boatz, J. A.; Elbert, S. T.; Gordon, M. S.; Jensen, J. J.; Koseki, S.; Matsunaga, N.; Nguyen, K. A.; Su, S.; Windus, T. L.; Dupuis, M.; Montgomery, J. A. *J. Comput. Chem.* **1993**, *14*, 1347.

(15) Malick, D. K.; Petersson, G. A.; Montgomery, J. A. *J. Chem. Phys.* **1998**, *108*, 5704; Petersson, G. A. Complete Basis Set Thermochemistry and Kinetics. In *Computational Thermochemistry: Prediction and Estimation of Molecular Thermodynamics*; Irikura, K. K., and Frurip, D. J., Eds.; ACS Symposium Series No. 677, 1998.

(16) Gonzalez, C.; Schlegel, H. B. *J. Phys. Chem.* **1989**, *90*, 2154; **1990**, *94*, 5523.

(17) Binkley, J. S.; Pople, J. A.; Hehre, W. J. *J. Am. Chem. Soc.* **1980**, *102*, 939; Gordon, M. S.; Binkley, J. S.; Pople, J. A.; Pietro, W. J.; Hehre, W. J. *J. Am. Chem. Soc.* **1982**, *104*, 2797.

(18) Ditchfield, R.; Hehre, W. J.; Pople, J. A. *J. Chem. Phys.* **1971**, *54*, 724; Hehre, W. J.; Ditchfield, R.; Pople, J. A. *J. Chem. Phys.* **1972**, *56*, 2257; Francl, M. M.; Pietro, W. J.; Hehre, W. J.; Binkley, J. S.; Gordon, M. S.; DeFrees, D. J.; Pople, J. A. *J. Chem. Phys.* **1982**, *77*, 3654.

(19) Hay, P. J.; Wadt, W. R. *J. Chem. Phys.* **1985**, *82*, 270.

(20) Stevens, W. J.; Bash, H.; Krauss, M. *J. Chem. Phys.* **1984**, *81*, 6026.

(21) Pietro, W. J.; Francl, M. M.; Hehre, W. J.; DeFrees, D. J.; Pople, J. A.; Binkley, J. S. *J. Am. Chem. Soc.* **1982**, *104*, 5039.

(22) Clark, T.; Chandrasekhar, J.; Spitznagel, G. W.; von R. Schleyer, P. *J. Comput. Chem.* **1983**, *4*, 294.

(23) Spitznagel, G. W. Diplomarbeit, Erlangen, 1982.

(24) The entire RC is consistent with $ClONO_2$ situated on an ice lattice in which HCl has *previously* ionized.[9]

(25) See, for example, Lee, T. J. *J. Phys. Chem.* **1995**, *99*, 1943.

(26) With the methodology described in Section II, the MP2 energy gap between planar $ClONO_2$ and its structure with the two Cl2−O3−N6−(O8,O3) dihedral angles constrained to be equal is ∼7.6 kcal/mol, indicating a hindered rotation around the O3−N6 axis.

(27) The MP2 RC and TS zero-point energies were calculated for the respective geometries at the HF/(HW*,3-21G) level by scaling the frequencies by 0.89 [Pople, J. A.; Schlegel, H. B.; Krishnan, R.; DeFrees, D. J.; Binkley, J. S.; Frish, M. J.; Whiteside, R. A.; Hout, R. S.; Hehre, W. J. *Int. J. Quantum Chem., Quantum Chem. Symp.* **1981**, *15*, 269]. The ZPE(TS)-ZPE(RC) difference is −0.97 kcal/mol.

(28) See, for example, Szabo, A.; Ostlund, N. S. *Modern Quantum Chemistry*; Dover Publications: Mineola, NY, 1996; p 152.

(29) Molina, M. J.; Tso, T. L.; Molina, L. T.; Wang, F. C. Y. *Science* **1987**, *238*, 1253.

(30) Gertner, B. J.; Whitnell, R. M.; Wilson, K. R.; Hynes, J. T. *J. Am. Chem. Soc.* **1991**, *113*, 74.

(31) Further, the prior solvation/desolvation features discussed above are consistent with those expected for a proton transfer reaction (see, for example, Ando, K.; Hynes, J. T. *J. Phys. Chem. B* **1997**, *101*, 10464).

(32) A gas-phase analogue has been described in ref 11.

(33) We believe that an H/D isotope is probably not observable for the $ClONO_2$ hydrolysis on ice despite the proposed proton transfer involvement,[13] due to the HOCl desorption energy (ca. 13 kcal/mol)[4] exceeding the calculated ∼3 kcal/mol reaction barrier;[13] the surface reaction would not then be rate limiting. The observed lack of an H/D isotope effect for $ClONO_2$ hydrolysis on D_2O ice supports this view (D. Hanson, personal communication). For reaction I.1, however, Cl_2 dissociation from the ice with accompanying increased NO_3^- solvation is exothermic (see text and ref 11), with the mechanism at a dynamic surface—Haynes, D. R.; Tro, N. J.; George, S. M. *J. Phys. Chem.* **1992**, *96*, 8502 and ref 9—likely being the simple exchange of an H_2O for the Cl_2 in the NO_3 solvation shell. Thus the barrier should be low to modest, such that the overall rate would still depend on the eq I.1 rate, with a resulting finite kinetic isotope effect.

(34) This calculated barrier value is close to estimates provided by several sources. See, for example, Berland, B. S.; Tolbert, M. A.; George, S. M. *J. Phys. Chem. A* **1997,** *101*, 9954, and references in ref 13.

(35) This important suppression is over and above any difficulty with the subsequent reaction eq I.3. Conflicting interpretations[6,13] have been advanced for the accessibility to reaction of the HOCl produced in eq I.2.

(36) See, for example, Chandrasekhar, J.; Smith, S. F.; Jorgensen, W. L. *J. Am. Chem. Soc.* **1984**, *106*, 3049; **1985**, *107*, 154.

(37) In a simple "solvation" view of the proton transfer, in connection with the S_N2 portion of the process in the eq I.1 mechanism found herein, the proton's presence could raise the S_N2 activation barrier compared to its absence in eq I.2. However, this view ignores the proton's important assisting electronic effects (Section IIIB.b).

(38) Bianco, R.; Hynes, J. T. Work in progress.

(39) Abbatt, J. P. D.; Molina, M. J. *J. Phys. Chem.* **1992**, *96*, 7674; Hanson, D. R.; Ravishankara, A. R. *J. Geophys. Res.* **1993**, *98*, 22,931; Zhang, R.; Jayne, J. T.; Molina, M. J. *J. Phys. Chem.* **1994**, *98*, 867.

(40) Differential solvation effects of H_2O and D_2O (Marcus, Y. *Ion Solvation*, Wiley: New York, 1985) would require attention in this connection.